RSC Advances

RSC Publishing

PAPER

View Article Online
View Journal | View Issue

Cite this: *RSC Advances*, 2013, **3**, 11832

Graphene oxide sheets as a template for dye assembly: graphene oxide sheets induce H-aggregates of pyronin (Y) dye†

Mehmet Şinoforoğlu, Bahri Gür, Mustafa Arık, Yavuz Onganer and Kadem Meral*

Received 30th January 2013,
Accepted 1st May 2013

DOI: 10.1039/c3ra40531a

www.rsc.org/advances

The highly stable colloidal structure of graphene oxide (GO) in aqueous dispersion behaves as a platform for the molecular aggregation of dyes *via* a simple adsorption process. The interaction between dye and GO sheets is a critical factor for dye aggregation. Positively charged dyes interact with the negatively charged GO sheets in an aqueous dispersion *via* both electrostatic and π–π stacking interactions. The cationic nature of Pyronin Y (PyY) ensures that the dye molecules are quickly adsorbed on the GO sheets in the aqueous dispersion. GO–PyY composites with different ratios, which are stable for months, are prepared by simply mixing diluted aqueous dispersions of both components. Transition dipole–dipole interactions between the adsorbed dye molecules on the surface of the GO sheet causes the formation of H-aggregates of the dye at dilute concentrations. H-aggregates of PyY are characterized by spectroscopic techniques (UV-Vis, steady-state and time-resolved fluorescence spectroscopy). The morphology and thickness of the GO sheets and the dye adsorbed GO sheets were determined using atomic force microscopy (AFM) in tapping mode. AFM studies revealed that a great deal of PyY molecules interact on the edges of the GO sheets.

1. Introduction

Out of various graphitic materials, graphene oxide (GO) is rapidly becoming one of the most popular research areas since graphene was first reported in 2004.[1] Its extraordinary mechanical and structural properties provide potential applications for GO in many fields such as electronic devices,[2] solar cells,[3] sensors,[4] adsorption,[5] Li-ion batteries,[6] supercapacitors[7] and hydrogen storage.[8] GO is a strongly oxygenated and highly layered material, which can be synthesized by facile chemical methods from pristine graphite.[1] In this regard, many routes for the synthesis of GO have been proposed by different research groups.[9,10] The chemical structure of GO has been widely investigated by theoretical and spectroscopic methods and it is generally concluded that the hydroxyl and epoxy groups mainly exist in the basal plane, while other functional groups, including carboxylic and carbonyl groups, are located at the edges.[4,9]

The high functionality and ease of modification of the GO surface originate from the variety of functional handles offered by these groups to organic molecules.[9,11,12] Considering the layered structure of GO, stable dispersions consisting mostly of single layer sheets in a polar solvent are obtained on a large scale by exfoliating from GO.[13] The electrostatic repulsion between GO sheets provides a stable aqueous dispersion because the surfaces of GO sheets have negative charges when dispersed in water.[11,14] The excellent colloidal stability of GO sheets enables them to be used in some technological applications as attractive surfaces.[4] As a result of this, organic and inorganic molecules and biomolecules can be physically adsorbed on the GO surface *via* strong π–π and electrostatic interactions.[15,16] Therefore, the GO sheets in aqueous dispersions can be used as a supporting platform for adsorbing a large amount of functional molecules.[15,16] For instance, GO sheets in an aqueous dispersion are an ideal platform for enzyme immobilization, which arises due to the interaction between the enzyme and the functional groups of GO.[16] Furthermore, GO sheets with a huge surface area are used as an adsorbent for the separation of many pollutants from aqueous solutions.[5,11]

In this sense, the extraordinary colloidal properties of GO sheets in aqueous dispersions may provide a platform for the formation of ordered structures of dye molecules, named dye aggregates. The formation and control of these dye structures are important because of the use of dye aggregates in some

Department of Chemistry, Ataturk University, Erzurum, 25240, Turkey. E-mail: kademm@atauni.edu.tr; Fax: +90442310948; Tel: +04422314410

† Electronic supplementary information (ESI) available: Synthesis of graphene oxide (GO), SEM image of natural graphite flakes, EDX spectra of natural graphite flakes and GO, Raman spectra of natural graphite flakes and GO, TGA spectra of natural graphite flakes and GO, cross-sectional analysis of AFM images of GO and PyY adsorbed GO on a mica surface, and absorption spectra of PyY in deionized water and the GO aqueous dispersion. See DOI: 10.1039/c3ra40531a

technological applications.[17,18] Molecular aggregates are formed by dipole–dipole interactions between dye monomers in aggregate units consisting of at least two monomers.[19] This specific interaction between dye monomers results in splitting and spectral shifting of the absorption spectra of the dye molecules compared to that of the free monomer. The numbers of dye monomers in the aggregate units affect the type and degree of dye aggregation. There are two main types of molecular aggregates depending on the type of intermolecular association, their structure, and their optical properties. Generally, H-aggregates (face-to-face arrangement of the monomer molecules in the unit) are characterized by a new blue-shifted absorption band compared to that of monomer whereas J-aggregates (side-by-side arrangement of the monomer molecules in the unit) possess a narrow and red-shifted absorption band. Owing to the discriminative absorption properties of molecular aggregates, they are easily characterized by UV-Vis absorption spectroscopy.[19] Furthermore, the luminescence properties of these aggregates are used as identification criteria, because H-aggregates quench the fluorescence intensity of the dye, while J-aggregates have a stronger emission intensity compared to that of monomeric dyes. Therefore, non-fluorescent H-aggregates decrease the quantum yield and fluorescence lifetime of the dye compared to that of the monomer.[17] The type of dye aggregate strongly depends on the molecular structure of the monomer. In this regard, it is well known that the aggregation ability of planar dye molecules is higher than that of the other dye molecules.[20] Pyronin Y (PyY) is a xanthene derivative dye with a planar structure which has found significant use in different research areas. Aggregate formation of the dye in different media has been determined by spectroscopic techniques, and the aggregate type was reported to be H-aggregate.[17,19–22] It was concluded that H-aggregate formation of PyY is observed at low dye concentrations in solution with certain additives such as clay, colloidal SiO_2 and sodiumdodecylsulphate (SDS), while aggregation of the dye takes place at high concentrations in water.[17,19–21] As a consequence of this observation, it can be said that the surface used as a template plays a crucial role in the aggregation processes of PyY. The role of the template is to form the ordered aggregates at low dye concentration, by utilizing the attractive surface force of the dye molecules. Therefore, we decided to use GO sheets as the template in the aggregation process of PyY dye molecules because they adsorb dye molecules from aqueous solution extremely well.

Herein, we show that GO sheets with colloidal stability in aqueous dispersion can be used as a platform for forming molecular assemblies on its surface. GO sheets bring about the formation of PyY aggregates even if the dye concentration is low. The obtained limpid solution containing GO–PyY composites are homogeneous and stable for months. The molecular aggregates of PyY were characterized with spectroscopic techniques such as UV-Vis, and steady state and time-resolved fluorescence spectroscopy. The GO sheet surface both with and without adsorbed dye was characterized by using tapping mode AFM.

2. Experimental section

2.1. Materials

Pyronin Y, Rhodamine 101 (used as reference for quantum yield), potassium permanganate ($KMnO_4$), hydrogen peroxide (H_2O_2, 30%), sodium nitrate ($NaNO_3$), and sulphuric acid (H_2SO_4, 98%) were purchased from Sigma-Aldrich. Natural graphite flakes (average particle size 325 mesh) were purchased from Alfa Aesar. All chemicals were used without further purification.

2.2. Characterization methods

TEM (transmission electron microscopy) images were obtained using a JEM-2100 (JEOL) instrument operating at 200 kV. SEM (scanning electron microscopy) images were acquired using a Zeiss EVO40. AFM (atomic force microscopy) images of the as-prepared thin films of GO and GO–PyY composite were captured in the air using Nanomagnetics instruments obtained from Ankara, Turkey.[23] The images were acquired in a tapping mode at room temperature. To prepare the thin films, GO and GO–PyY composite in an aqueous solution were spin-coated onto a freshly cleaved mica substrate at 3000 rpm (60 s) and the samples were left more than 24 h in order to evaporate the solvent. Absorption spectra were recorded on a Perkin-Elmer (Model Lambda 35) spectrophotometer at room temperature. Steady-state fluorescence spectra of the sample were taken by a Shimadzu RF-5301 PC spectrofluorophotometer. The observed fluorescence spectra were converted to corrected fluorescence spectra.[20] Fluorescence decays to measure the fluorescence lifetime were carried out with a Laser Strobe Model TM-3 lifetime fluorometer (Photon Technology International). The excitation source consisted of a pulsed nitrogen laser–tunable dye laser combination. Pulse width is about 800 ps and has repetition rate of up to 20 pulses per second. The decay curves were collected over 200 channels using a nonlinear time scale with the time increment increasing according to the arithmetic progression. The fluorescence decay was analyzed with the lifetime distribution analysis software from the instrument supplying company. Fluorescence quantum yields (Φ_f) of the samples were calculated by comparison with a reference solution. Rhodamine 101 (Rh101) (Φ_f = 1.0 in ethanol) was used as the reference dye. Fluorescence quantum yields of PyY in the GO dispersion were determined according to the following equation;

$$\Phi_f = \Phi_{f,ref} (A_{ref}/A) (n_D/n_{D,ref})^2 (\alpha_D/\alpha_{D,ref}) \quad (1)$$

where $\Phi_{f,ref}$ is the fluorescence quantum yield of the reference compound, A is the absorbance, n_D is the index of refraction of the solvent, and α is the area under the corrected fluorescence peak. All measurements related to absorption and fluorescence studies were recorded using 1.0 cm quartz cuvettes.

2.3. Synthesis of GO

GO was synthesized using the modified Hummer's method.[8] Details of the synthesis and characterization of the GO are presented in the Supporting Information (Fig. S1–S5, ESI†). TEM and SEM images of GO are shown in Fig. 1. The many

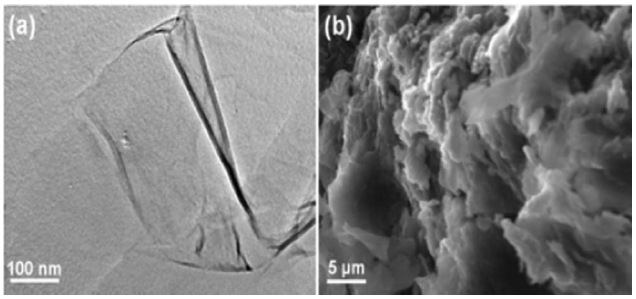

Fig. 1 TEM (a) and SEM (b) images of a GO sheet.

wrinkles in the TEM image suggest the formation of GO. Additionally, it can be readily seen from the SEM images of graphite (Fig. S1, ESI†) and GO (Fig. 1b) that the smooth leaf structure of the graphite flakes was completely changed into a rough and porous structure after oxidation in a strong acidic medium. The oxidation of natural graphite flakes to form GO was confirmed by EDX (energy dispersive X-ray) studies (Fig. S2 and S3, ESI†).

2.4. Preparation of stable GO dispersions

GO was dispersed in water to an average concentration of 1.0 mg mL^{-1} with the aid of an ultrasonication bath for 3 h. After several sonication processes, the dispersions were allowed to settle for several weeks at room temperature. In the meantime, the water-insoluble and bigger sheets of GO settled due to gravity forces and the limpid GO dispersion was carefully separated by decantation processes. In this way, the obtained GO stock dispersion was made homogenous and was stable for months. In this dispersion, the amount of GO was determined to be 0.85 mg mL^{-1}. The GO dispersion (0.85 mg mL^{-1}) was diluted to make various GO aqueous dispersions.

2.5. Preparation of GO–PyY composites in aqueous dispersions

Dye samples were prepared from fresh stock solutions of concentrated PyY (1.0×10^{-3} M) in ethanol. After a given volume of the PyY sample was transferred into a flask, the solvent was evaporated by argon gas purging, then 5.0 ml of GO dispersion was added into the flask containing PyY. The dye concentrations for the GO–PyY composites are presented in the figures. An appropriate amount of GO for the intense molecular aggregation of PyY in aqueous dispersion was determined to be 17 mg L^{-1} by means of UV-Vis study.

3. Results and discussion

3.1. Highly stable GO–PyY composites

Organic–inorganic composites were prepared by two substances incorporated in aqueous solution. Therefore, this method is facile and suitable for composite formation, including functional organic molecules and graphitic material. GO sheets in an aqueous dispersion are negatively charged because of the oxygenated groups of GO, such as carboxyl groups at the edge sites and hydroxyl groups on the basal plane. This supports both highly stable GO dispersion,

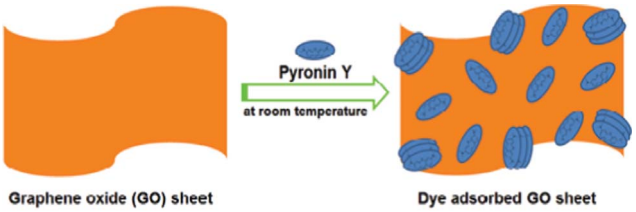

Scheme 1 Schematic illustration of a 2D GO–PyY nanocomposite in an aqueous dispersion.

as the steric hindrance and electrostatic repulsion caused by these negatively charged groups can excellently prevent the self-assembly of GO sheets, and easy binding with positively charged species.[4] In this regard, the cationic PyY molecules can be assembled onto the surfaces of the GO sheets through electrostatic and π–π stacking cooperative interactions.[15] This phenomenon is schematically represented in Scheme 1 by considering the spectroscopic and microscopic results.

AFM is widely used to determine the morphology of GO and its composites.[16] In this regard, the adsorption of PyY on GO sheets, that contain 1.0×10^{-5} M of dye and 17 mg L^{-1} of GO, and the morphology of the PyY–GO composite were monitored using AFM (Fig. 2). The AFM images show that the thicknesses of the GO sheets on a freshly prepared mica surface are ~1.0 nm, while the thickness of the GO–PyY composite is found to be ~1.4 nm (Fig. S6, ESI†). The AFM height image (Fig. S6b, c, ESI†) confirmed the noncovalent attachment of the PyY molecules on the GO sheets through π–π interactions as well as electrostatic interactions. Moreover, the intense assembly of the dye molecules at the edges of the GO sheet, where the thickness of the composite was found to be ~3.0 nm, can be clearly seen from the AFM images (Fig. S6c, ESI†). Consequently, the AFM studies revealed that the edges of GO (ionizable carboxyl groups) play a crucial role in the molecular assembly of PyY in the aqueous dispersion. This observation implies that cationic PyY molecules are adsorbed mainly by electrostatic forces onto GO sheets.

To date, many manuscripts have been published about the composite formation of organic molecules–GO sheets and their interaction forces.[15,24,25] For example, it was reported that reduced GO sheets complex with positively charged 5,10,15,20-tetrakis(1-methyl-4-pyridinio)porphyrin (TMPyP) in aqueous dispersions and the main driving forces in the

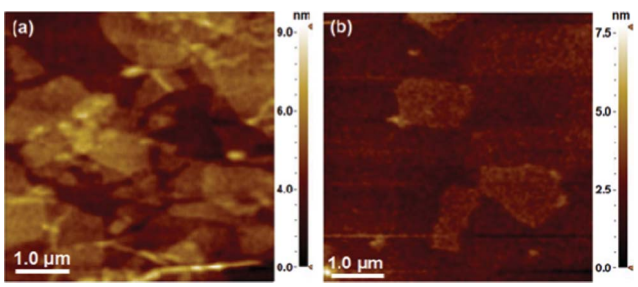

Fig. 2 Tapping mode AFM images (5 μm × 5 μm) of GO (a) and PyY adsorbed GO (b) on a freshly prepared mica surface.

composite structure consist of the electrostatic and π–π interactions between the TMPyP molecules and GO sheets.[15] The amount of dye in the GO–PyY composite plays a significant role in the stability of the colloidal dispersions. At higher dye concentrations, the stability of the GO–PyY composites in aqueous dispersion is destroyed, while the surface charge of the GO may approach neutral due to dye molecules adsorbed onto the GO surface. Subsequently large clusters of the GO–PyY composites start forming. In the present study, the highest dye concentration for stable composite formation in an aqueous dispersion of 17 mg L^{-1} of GO was determined to be 5.0 × 10^{-5} M.

3.2. Aggregation of PyY on GO sheets

3.2.1. The effect of the amount of GO. Since the amount of template material plays a critical role in the molecular aggregation process, the determination of its optimal condition is necessary. The optimum amount of GO sheets in aqueous dispersion was sensitively determined by absorption spectroscopy for the aggregation of PyY on GO. The solutions of PyY, with a concentration of 1.0 × 10^{-5} M, were prepared with various amounts of GO in aqueous dispersion. The aggregation tendency of PyY onto GO sheets was then followed by the obtained absorption spectra (Fig. 3).

The as-prepared GO–PyY composites, by varying the amount of GO, are homogeneous and stable for several months. At such a dye concentration, the PyY molecules have an intense absorption band at 546 nm in water, which is assigned to an isolated molecule (*i.e.* a dye monomer), as can be seen in Fig. 3. In contrast, the absorption spectra of PyY in the various GO aqueous dispersions are different than that in water. In the various GO aqueous dispersions, PyY has new absorption bands in the blue region as well as the monomer band, which are attributed to the dye associating as dimers and higher ordered aggregates. In Fig. 3, the more blue-shifted absorption band at ~480 nm indicates higher aggregates of the dye (H-aggregates) while the bands about at ~520 nm are attributed to the dimer (H-dimer). The π–π and electrostatic cooperative interactions between the PyY molecules and GO sheets lead to the perfect orientation of dyes as H-aggregates.[25] Taking into account the absorption spectra of 1.0 × 10^{-5} M PyY in the GO aqueous dispersions, dye aggregation in the dispersion with lower amounts of GO (>3.4 mg L^{-1}) is predominant, while the dye molecules were found to be monomeric in the concentrated GO aqueous dispersions (Fig. 3). Consequently, the GO aqueous dispersion containing 17 mg L^{-1} GO, where a perfect aggregate absorption band of PyY was observed, was selected for the aggregation study of the dye. The attachment of PyY molecules to GO sheets was confirmed using the results from UV-Vis spectroscopy studies (Fig. 3). Therefore, the nanoclusters formed at the edges of the GO sheets in the AFM images (Fig. S6c, ESI†) are attributed to the H-aggregates of PyY.

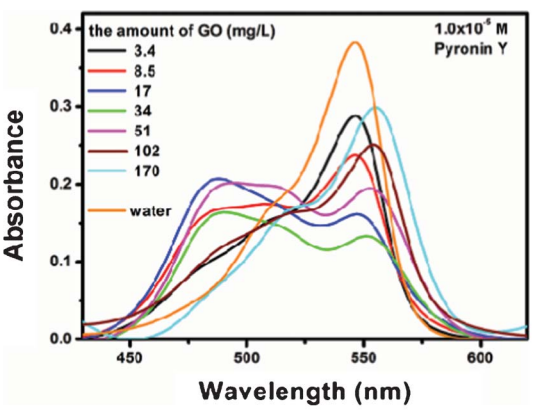

Fig. 3 The absorption spectra of PyY in various GO aqueous dispersions and water.

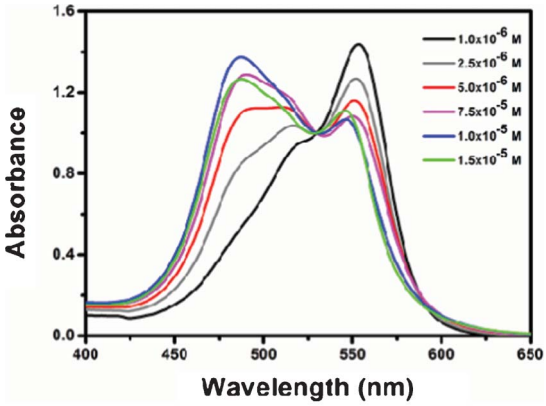

Fig. 4 The absorption spectra of PyY in the GO aqueous dispersion at various dye concentrations. (The GO aqueous dispersion includes 17 mg L^{-1} GO. The spectra were normalized at the isosbestic point in order to show clearly the change of relative absorbance due to monomers and aggregates.)

3.2.2. Photophysical properties of PyY in GO aqueous dispersions. The absorption characteristics of functional dye molecules such as pyronin dyes in aqueous solution or the solid state are strongly dependent on increasing the dye concentration, which is a driving force in forming dye aggregates. In this regard, UV-Vis spectroscopy allows determination of the molecular behavior of the dye as a function of increasing dye concentration. Fig. 4 shows the absorption spectra of PyY in a 17 mg L^{-1} GO aqueous dispersion at various dye concentrations.

As can be seen from Fig. 4, the shape of the absorption spectrum of PyY in the GO dispersion greatly depends on the dye concentration. At dilute dye concentrations (10^{-6} M), the intense absorption band appeared at 553 nm, which is attributed to the adsorbed dye monomers on the GO sheets in aqueous dispersions. By increasing the dye concentration, a new absorption band arose in the blue region, compared to the monomer absorption band, while decreasing the monomer band intensity. As the dye concentration reached 2.5 × 10^{-6} M, two absorption bands at ~490 nm and ~515 nm were existed as well as the monomer band. The absorption band at ~490 nm is attributed to H-aggregates of PyY, whilst the other band at 515 nm represents the dimer of the dye (referred to as the H-dimer). The effect of increasing the dye concentration on the absorption spectra of PyY in the GO aqueous dispersion was studied in the range of 1.0 × 10^{-6} M to 1.5 × 10^{-5} M. In

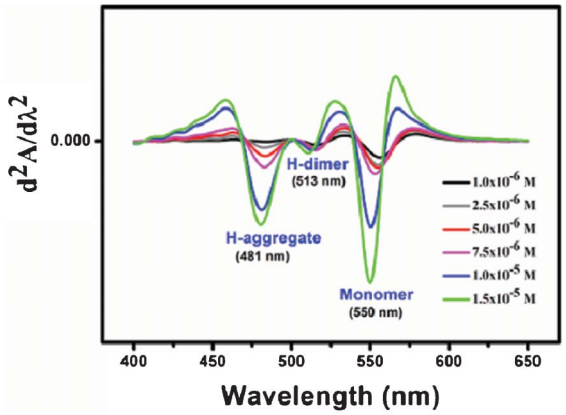

Fig. 5 The second derivative spectra of PyY in the GO dispersion.

this concentration range, the dimer band of the dye molecules is formed at moderate dye concentrations and is also more intense than the H-aggregate band. Further increasing the dye concentration leads to increasing formation of higher aggregates of the dye as can be seen from Fig. 4. This result reveals that there is an equilibrium between the monomer and the dye aggregate. At 1.0×10^{-5} M, the H-aggregate band of PyY reached a maximum as previously explained. Interestingly, further increasing the dye concentration ($>1.0 \times 10^{-5}$ M) results in an increase in the monomer absorption band intensity (Fig. S8, ESI†), and the absorption band of the monomer shifts to a higher energy region. Taking into account Fig. 4, the molecular associations onto the GO sheets is summarized below;

$$\text{Dye} + \text{Dye} \rightleftharpoons \text{Dimers} \rightleftharpoons \text{H-aggregates}$$

The strong interactions between the dye and the GO sheets in aqueous solution cause dye aggregation to take place at very low concentrations, while PyY molecules in water form H-aggregates starting at 1.0×10^{-4} M.[17] The intense aggregation of PyY in the concentration range studied is attributed to the localized high dye concentration at the edge sites of the GO sheets (Fig. 2b and Fig. S6c, ESI†). The seeming decrease in dye aggregation at high concentrations ($>1.0 \times 10^{-5}$) is due to the weak interaction between the dye-saturated GO surface and the dye molecules. The surface of GO is fully covered with dye molecules at this dye concentration, thereby leaving no sites for strong adsorption. The number of free dye monomers in the GO dispersion therefore increases at higher concentrations. The characteristics of the growing absorption band actually resemble those of the monomer absorption in water (Fig. S9, ESI†).

The absorption band maxima of dye compounds could not be defined clearly when the intense dye aggregation took place. The second derivative spectra of the samples were used for the characterization of overlapping absorption bands. The second derivative spectra of PyY in the GO aqueous dispersion depending on the dye concentration are presented in Fig. 5. As can be seen in Fig. 5, the monomer, H-dimer and H-aggregate band maxima of 1.0×10^{-5} M PyY in the GO dispersion were found to be 550 nm, 513 nm and 481 nm, respectively. It is clearly observed from Fig. 5 that the band maxima of the monomer, dimer and H-aggregate of PyY depending on the aggregation degree, where the strong dipole–dipole interactions between the monomers in the aggregate unit alter the exciton splitting energy, are changed (Table 1).

The decomposition of the aggregate spectrum of PyY into components also allows the determination of the aggregate geometry (Fig. 6). The H-aggregate of PyY in the GO aqueous dispersion was evaluated using a model in which the monomers are in parallel planes with a twist angle α with respect to the transition dipole moments of each monomer in the aggregate unit.[20] According to this approach, when $\alpha > 54.7^\circ$, H-aggregates are formed and when $\alpha < 54.7^\circ$, J-aggregates are formed. The angle for PyY calculated from the spectroscopic data was determined to be 78.4° and compatible with the literature value for H-aggregates of PyY.[20] Additionally, the band positions found in the deconvoluted spectrum of PyY are consistent with those found in the second derivative spectra.

Since this type composite is an appropriate structure for energy conversion systems, it is necessary to determine the fluorescence properties of the GO–PyY composites in aqueous dispersion. The fluorescence spectra of PyY at various GO/dye ratios in the aqueous dispersion were recorded at 500 nm excitation wavelength. PyY in water at dilute concentrations is strongly fluorescent, where the band maximum is located at 570 nm.[20] It is well-known that when the dye aggregation occurs, the fluorescent properties of dye are drastically changed in comparison with the monomer. The presence of non-fluorescent dye aggregates (H-aggregates and dimers) decreases the fluorescence intensity of the dye molecules due to the fast internal conversion process, in which the radiative transition from an excited state to a ground state is

Table 1 Absorption band maxima, quantum yields and fluorescence lifetimes of PyY in the GO aqueous dispersions[a]

[PyY] (μM)	Monomer (nm)	H-dimer (nm)	H-aggregate (nm)	Φ_f	τ (ns)	χ^2
1.0	556	516	—	0.056	1.50	1.1
2.5	555	516	483	0.044	1.30	1.0
5.0	555	516	483	0.039	1.25	1.1
7.5	553	515	483	0.040	1.32	1.1
10.0	550	513	481	0.062	1.33	1.1
15.0	550	511	481	0.079	1.43	1.0

[a] The absorption band maxima were obtained from the second derivative spectra.

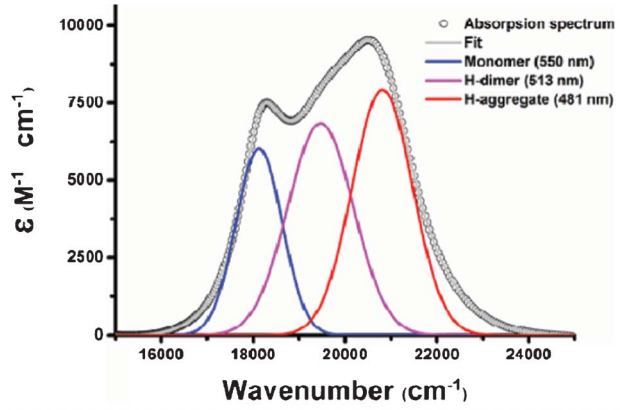

Fig. 6 Deconvolution of the aggregate absorption spectrum of 1.0 × 10^{-5} M PyY in the GO aqueous dispersion.

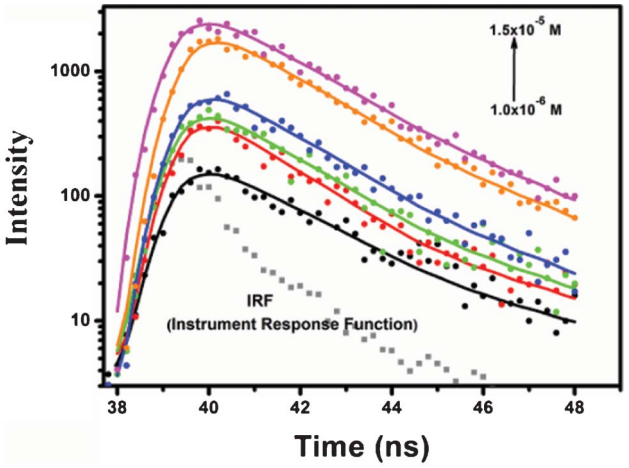

Fig. 8 Fluorescence decays and their exponential fits for PyY in the GO aqueous dispersion with varying dye concentration.

forbidden.[17] In this regard, the fluorescence properties of the various GO–PyY composites, which have different absorption properties, are investigated in the aqueous dispersion (Fig. 7). The main bands at 558 nm were obtained for all GO–PyY composites at room temperature (Fig. 7). These fluorescence bands originated from the monomeric PyY being adsorbed onto GO sheets in the aqueous dispersion because H-aggregates and dimers are non-fluorescent species.

According to the performed fluorescence studies in water and GO aqueous dispersions, the fluorescence intensity of PyY in the aqueous dispersion is lower compared to that found in water at the same dye concentrations. This phenomenon is attributed to the non-fluorescent aggregates and the quenched fluorescence properties of the GO sheets.[26] The fluorescent efficiency of the PyY molecules in the aqueous dispersion is evaluated by quantum yields. The non-fluorescent aggregates of the dye and the presence of the GO sheets strongly affect the quantum yield of PyY (Table 1). The quantum yield of PyY in water is very high and was found to be 0.47.[27] The calculated quantum yields of PyY in the GO aqueous dispersion are very low compared to that found in water.

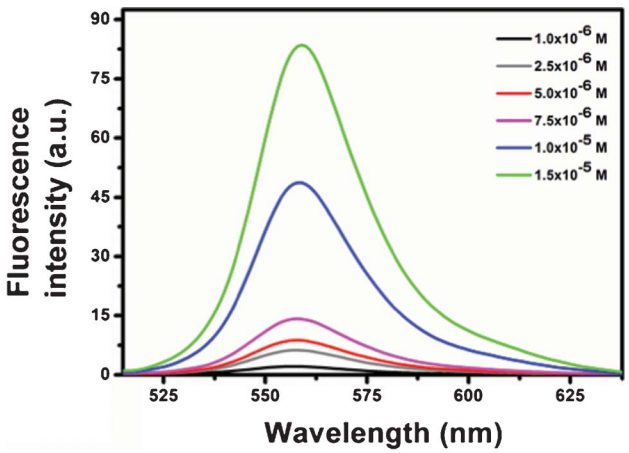

Fig. 7 The fluorescence spectra of PyY in the GO dispersion at various dye concentrations. (The GO aqueous dispersion includes 17 mg L^{-1} GO.)

To determine the fluorescence lifetime of PyY in the GO aqueous dispersion, fluorescence decay spectra of PyY were recorded upon excitation at 500 nm. The fluorescence decay spectra of PyY in the GO aqueous dispersion are presented in Fig. 8. According to the exponential analyses, it was found that the fluorescence decay of PyY in the GO aqueous solution has single-exponential decay kinetics because of the acceptable statistical χ^2 values. The single-exponential decay kinetics indicate a homogeneous environment around the fluorescent dye molecules. The fluorescence lifetime of PyY in water, where the dye is in the monomeric form, was reported to be 1.79 ns.[21] From Table 1, the fluorescence lifetime of PyY in the GO aqueous dispersion is decreased when the dye is both monomeric and H-aggregated in structure.

Because H-aggregates quench the fluorescence intensity and decrease the fluorescence lifetime of the species, the decrease in the fluorescence lifetime of PyY is acceptable in the presence of H-type aggregates in the aqueous dispersion. The fluorescence lifetime of PyY in the monomeric form in the GO aqueous dispersion is lower than that found in water, and confirms that the GO is a fluorescence quencher.[26] Additionally, the increase in both the fluorescence lifetime and quantum yield of PyY at concentrations beyond 5.0 × 10^{-6} M is ascribed to the altered interaction strength of GO–PyY, as previously discussed.

4. Conclusions

In the present study, GO–PyY composites at various GO/dye ratios, which are stable for several months, are prepared by simply mixing the diluted aqueous solutions of both components. It is determined that the stability of the composites in the aqueous dispersion is dependent on dye concentration. The attractive surface of the GO sheets for the dye molecules rapidly generates the GO–PyY composites in the aqueous

dispersion. The strong electrostatic interaction between the negatively charged GO sheets and cationic dye molecules as well as π–π interactions induce the adsorption of PyY onto the GO surface. As a result of this fast adsorption, well-organized structures of PyY are formed on the GO sheets at dilute dye concentrations due to the localized high dye concentration. AFM study confirms the dye adsorption on the GO and also demonstrates the huge adsorption of the dye on the edges of the GO sheets. Spectroscopic studies reveal that the amount of GO in the aqueous dispersion plays an important role in the aggregation of PyY, and the optimum amount was determined to be 17.0 mg L^{-1}. H-aggregates of PyY on GO sheets are formed with increasing dye concentration. The presence of intense H-type aggregation decreases the quantum yield and fluorescence lifetime of PyY. Consequently, certain amounts of GO in the aqueous dispersion are used as a template to form functional dye assemblies. The facile preparation of the GO–dye composites has a remarkable impact in material chemistry because both dye compounds and their well-ordered structure are used in many technological areas.

Acknowledgements

The financial support by ''Atatürk University Scientific Research ''Project Council (Project No: 2012/467)'' is gratefully acknowledged.

References

1 Y. Zhu, D. K. James and J. M. Tour, *Adv. Mater.*, 2012, **24**, 4924.
2 S. Petersen, M. Glyvradal, P. Bøggild, W. Hu, R. Feidenhans'I and B. W. Laursen, *ACS Nano*, 2012, **6**, 8022.
3 R. Narayanan, M. Deepa and A. K. Srivastava, *Phys. Chem. Chem. Phys.*, 2012, **14**, 767.
4 J. Balapanuru, J. Yang, S. Xiao, Q. Bao, M. Jahan, L. Polavarapu, J. Wei, Q. Xu and K. P. Loh, *Angew. Chem.*, 2010, **122**, 6699.
5 G. K. Ramesha, A. V. Kumara, H. B. Muralidhara and S. Sampath, *J. Colloid Interface Sci.*, 2011, **361**, 270.
6 X. Zhu, Y. Zhu, S. Murali, M. D. Stoller and R. S. Ruoff, *ACS Nano*, 2011, **5**, 3333.
7 L. L. Zhang, X. Zhao, M. D. Stoller, Y. Zhu, H. Ji, S. Murali, Y. Wu, S. Perales, B. Clevenger and R. S. Ruoff, *Nano Lett.*, 2012, **12**, 1806.
8 Ö. Metin, E. Kayhan, S. Özkar and J. J. Schneider, *Int. J. Hydrogen Energy*, 2012, **37**, 8161.
9 D. R. Dreyer, S. Park, C. W. Bielawski and R. S. Ruoff, *Chem. Soc. Rev.*, 2010, **39**, 228.
10 D. C. Marcano, D. V. Kosynkin, J. M. Berlin, A. Sinitskii, Z. Sun, A. Slesarev, L. B. Alemany, W. Lu and J. M. Tour, *ACS Nano*, 2010, **4**, 4806.
11 S. Park and R. S. Ruoff, *Nat. Nanotechnol.*, 2009, **4**, 217.
12 Z. Lin, Y. Liu and C. Wong, *Langmuir*, 2010, **26**, 16110.
13 J. I. Paredes, S. Villar-Rodil, A. Martinez-Alonso and J. M. D. Tascon, *Langmuir*, 2008, **24**, 10560.
14 X. Wang, H. Bai and G. Shi, *J. Am. Chem. Soc.*, 2011, **133**, 6338.
15 Y. Xu, L. Zhao, H. Bai, W. Hong, C. Li and G. Shi, *J. Am. Chem. Soc.*, 2009, **131**, 13490.
16 J. Zhang, F. Zhang, H. Yang, X. Huang, H. Liu, J. Zhang and S. Guo, *Langmuir*, 2010, **26**, 6083.
17 B. Gür and K. Meral, *Spectrochim. Acta, Part A*, 2013, **101**, 306.
18 A. Chowdhury, S. Wachsmann-Hogiu, P. R. Bangal, I. Raheem and L. Peteanu, *J. Phys. Chem. B*, 2001, **105**, 12196.
19 K. Meral, N. Yılmaz, M. Kaya, A. Tabak and Y. Onganer, *J. Lumin.*, 2011, **131**, 2121.
20 M. Arık and Y. Onganer, *Chem. Phys. Lett.*, 2003, **375**, 126.
21 M. Arık, K. Meral and Y. Onganer, *J. Lumin.*, 2009, **129**, 599.
22 K. Meral, H. Y. Erbil and Y. Onganer, *Appl. Surf. Sci.*, 2011, **258**, 1605.
23 B. Gür and K. Meral, *ColloidsSurf., A*, 2012, **414**, 281.
24 J. Barkauskas, I. Stankevicien, J. Daksevic and A. Padarauskas, *Carbon*, 2011, **49**, 5373.
25 K. Haubner, J. Murawski, P. Olk, L. M. Eng, C. Ziegler, B. Adolphi and E. Jaehne, *ChemPhysChem*, 2010, **11**, 2131.
26 Y. Liua, C. Liua and Y. Liu, *Appl. Surf. Sci.*, 2011, **257**, 5513.
27 J. Bordello, B. Reija, W. Al-Soufi and M. Novo, *ChemPhysChem*, 2009, **10**, 931.

